

Quasar Absorption Lines in the Far Ultraviolet: An Untapped Gold Mine for Galaxy Evolution Studies

Todd M. Tripp [tripp@astro.umass.edu, (413)-545-3070]

Department of Astronomy, University of Massachusetts-Amherst, Amherst, MA 01003

ABSTRACT

Most of the baryons are exceedingly difficult to observe, at all epochs. Theoretically, we expect that the majority of the baryonic matter is located in low-density, highly ionized gaseous envelopes of galaxies – the “circumgalactic medium” – and in the highly ionized intergalactic medium. Interactions with the CGM and IGM are thought to play crucial roles in galaxy evolution through accretion, which provides the necessary fuel to sustain on-going star formation, and through feedback-driven outflows and dynamical gas-stripping processes, which truncate and regulate star formation as required in various contexts (e.g., low-mass vs. high-mass galaxies; cluster vs. field). Due to the low density and highly ionized condition of these gases, quasar absorption lines in the rest-frame ultraviolet and X-ray regimes provide the most efficient observational probes of the CGM and IGM, but ultraviolet spectrographs offer vastly higher spectral resolution and sensitivity than X-ray instruments, and there are many more suitable targets in the UV, which enables carefully designed studies of samples of particular classes of objects. This white paper emphasizes the potential of QSO absorption lines in the rest-frame far/extreme UV at $500 \lesssim \lambda_{\text{rest}} \lesssim 2000 \text{ \AA}$. In this wavelength range, species such as Ne VIII, Na IX, and Mg X can be detected, providing diagnostics of gas with temperatures $\gg 10^6 \text{ K}$, as well as banks of adjacent ions such as O I, O II, O III, O IV, O V, and O VI (and similarly N I – N V; S II – S VI; Ne II – Ne VIII, etc.), which constrain physical conditions with unprecedented precision. A UV spectrograph with good sensitivity down to observed wavelengths of 1000 \AA can detect these new species in absorption systems with redshift $z_{\text{abs}} \gtrsim 0.3$, and at these redshifts, the detailed relationships between the absorbers and nearby galaxies and large-scale environment can be studied from the ground. By observing QSOs at $z = 1.0 - 1.5$, *HST* has started to exploit extreme-UV QSO absorption lines, but *HST* can only reach a small number of these targets. A future, more sensitive UV spectrograph could open up this new discovery space.

1. QSO Absorption Lines at Wavelengths $< 912 \text{ \AA}$

High-resolution ultraviolet spectroscopy provides a unique ability to study low-density gas/plasma in galaxy disks, halos, and the intergalactic medium (IGM), i.e., all harbors of present-epoch baryons. Since stars account for only a small fraction of the baryon inventory and most of the ordinary matter is in very low-density gases (Fukugita et al. 1998, ApJ, 503, 518), UV spectroscopy is a crucial technique for the study of galaxy ecosystems and the cycles of inflowing and outflowing matter and energy that regulate galaxy formation. As anticipated by Verner et al. (1994, ApJ, 430, 186), the deployment of the *Cosmic Origins Spectrograph* (COS, Green et al. 2012, ApJ, 744, 60) on the *Hubble Space Telescope* has demonstrated a particularly powerful new window for UV spectroscopy: the study of QSO absorption lines in the “extreme” ultraviolet (EUV) at $\lambda < 912 \text{ \AA}$. Normally, we assume that EUV absorption lines cannot be observed because the Galactic ISM prevents observations of transitions at these wavelengths in the Milky Way. However, if gas in a quasar absorption system has a sufficiently high redshift, these lines are redshifted into the *HST* bandpass; for example, the Ne VIII doublet at $770.4, 780.3 \text{ \AA}$ can be studied in QSO absorbers with redshift $z_{\text{abs}} \geq 0.3$ with a spectrograph sensitive down to 1000 \AA . Unfortunately, in very high-redshift QSO absorbers that can be observed from the ground, these EUV lines are ruined by blending with the thick Ly α forest. However, as illustrated in Figure 1, QSOs at $z \approx 1 - 1.5$ are in a “sweet spot” where the EUV lines can be detected but the line density is low enough so that blending is not severe. These COS data demonstrate the potential of EUV lines, but unfortunately, HST+COS can only access a small number of these targets in reasonable exposure times. Moreover, while the COS spectra have signal-to-noise $\approx 30 - 50$ per resel, higher S/N ($\gtrsim 100$) would greatly improve this technique because the key lines (e.g., Ne VIII) can be quite weak (see, e.g. Meiring et al. 2012, arXiv1201.0939).

Figure 2 demonstrates the following unique diagnostics provided by EUV absorption spectroscopy: First, EUV absorption lines include species such as Ne VIII, Mg X, and Si XII, and these species are detectable in plasmas at $T > 10^6 \text{ K}$. Thus, in the EUV, *HST* can compete with X-ray telescopes, but *HST* has much better spectral resolution, better sensitivity, and a substantially larger pool of sufficiently bright targets, which enables more optimal target selection. The Astro2010 decadal survey identified the *International X-ray Observatory* as a top priority for the next 20 years, and one of the prime science drivers of IXO is the study of missing baryons and hot gas in low-density gaseous halos and the IGM using absorption spectroscopy. By using species such as Ne VIII and Mg X, we can pursue this IXO science goal immediately. We have already successfully detected Ne VIII, Mg X, and other highly ionized hot-gas tracers (see below). Second, the EUV includes transitions of suites of adjacent ions such as O I, O II, O III, O IV, O V, and O VI or S II, S III, S IV, and S V (similar sets are available for C, N, etc). These adjacent ions span a wide range of

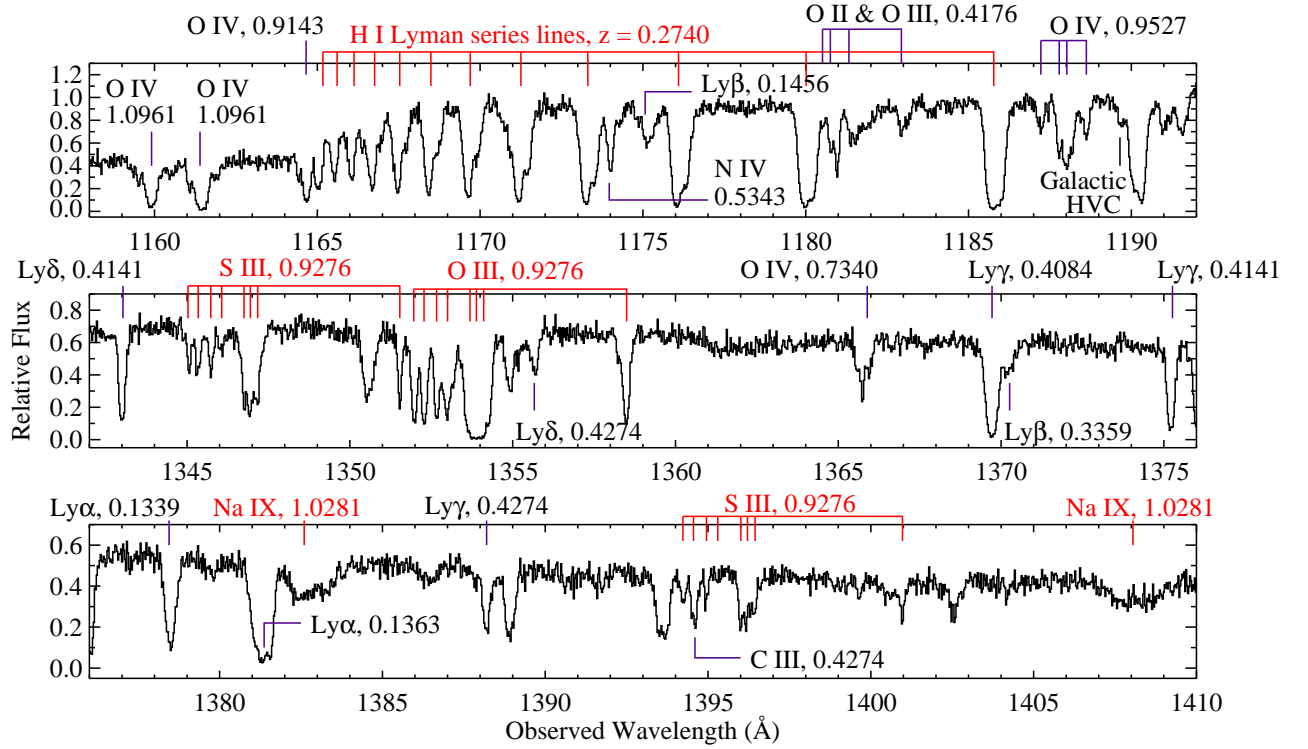


Fig. 1.— Examples of the COS spectra obtained from our *Hubble Space Telescope* program from the sight lines to PG1630+377 ($z_{\text{QSO}} = 1.476$, top panel) and PG1206+459 ($z_{\text{QSO}} = 1.163$ middle and lower panels). Various lines of metals and H I are labeled with their redshifts. **Most of the lines in this figure have rest-frame wavelengths $< 912 \text{ \AA}$; the shortest-wavelength transitions shown here are the Na IX doublet with $\lambda_{\text{rest}} = 681.7, 694.3 \text{ \AA}$ and the O IV lines at $\lambda_{\text{rest}} = 553.3, 554.1 \text{ \AA}$.** Lines and systems of particular interest are indicated in red. The high S/N of these data and access to lines down to the H I Lyman limit (and beyond) provide very precise constraints on the H I column densities, the ionization state of the gas, the metallicity, gas kinematics, and insights on the multiphase physics that governs circumgalactic and intergalactic gases. Note that these are only small portions of the spectrum for each quasar and are representative of the full sample.

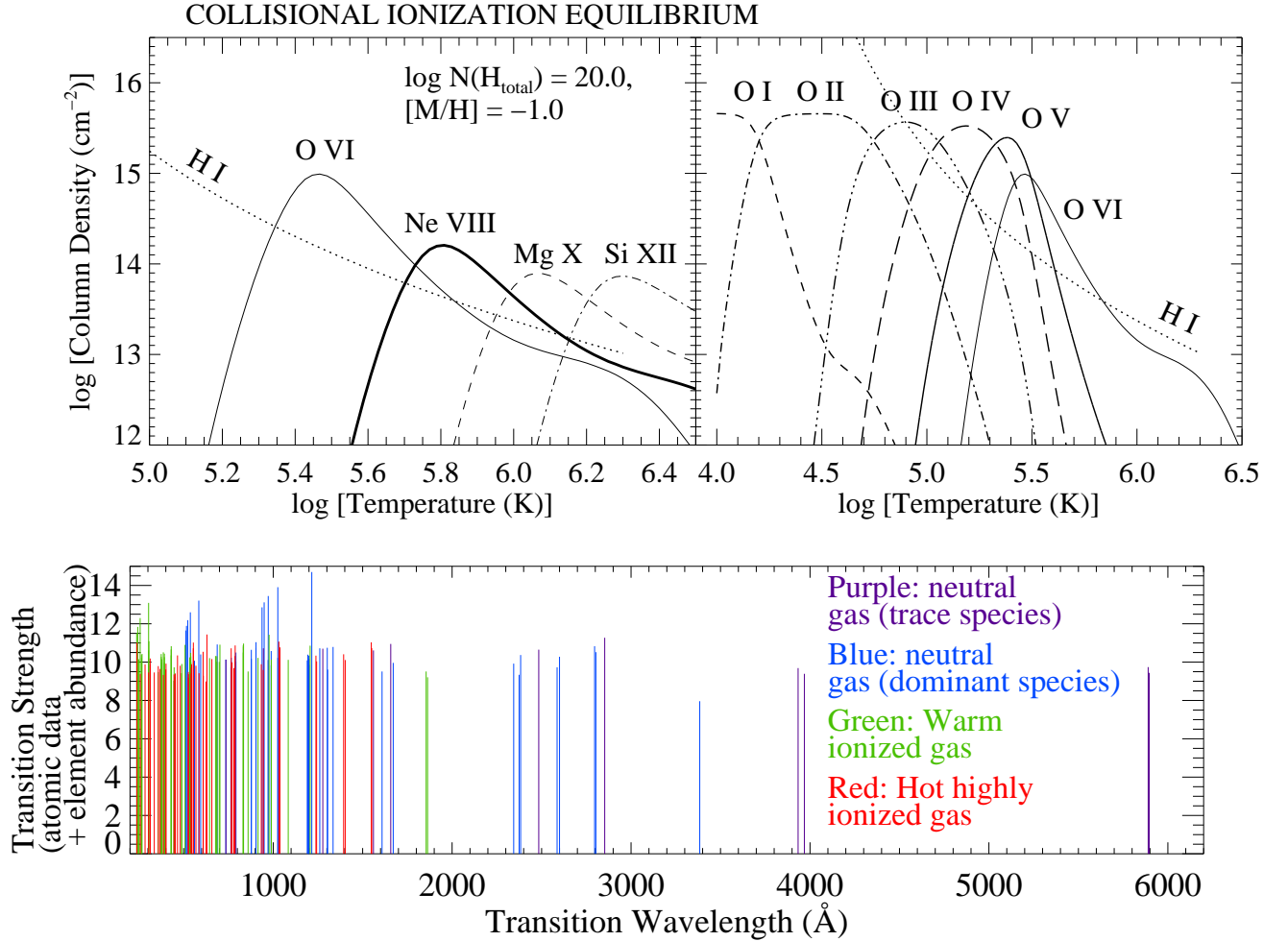


Fig. 2.— *Upper panels:* Column densities of various metals in collisional ionization equilibrium, as a function of temperature, for an absorber with $N(\text{H}_{\text{total}}) = 10^{20} \text{ cm}^{-2}$ and $Z = 0.1Z_{\odot}$. *Lower panel:* Strength of resonance lines vs. the rest-frame wavelength of the transition from Verner et al. (1994, A&AS, 108, 287) based on the element abundance and atomic data (taller lines indicate intrinsically stronger transitions). Colors indicate tracers of difference gas phases (see legend). In addition to providing access to a larger number of sight lines, a future UV spectroscopic facility with greater sensitivity could more effectively exploit the rich diagnostics available at $\lambda < 1000 \text{ \AA}$ by detecting weaker lines with higher signal-to-noise spectra.

temperatures/ionization conditions (see Fig. 2), and limits on or detections of these species can constrain the physics and metallicity of QSO absorbers with unprecedented precision [note that currently, we typically only have access to scattered ionization stages such as O VI, C III, and Si III in low- $N(\text{H I})$ absorbers]. As shown in the lower panel of Fig. 2, the EUV is the richest region of the spectrum for QSO absorption spectroscopy. Third, the redshifts of the absorbers are sufficient to bring many H I Lyman series lines into the *HST* band (see examples in Figure 1). This enables accurate H I column-density measurements because the higher Lyman series lines are less likely to be saturated. Observations of lower-redshift absorbers often detect only a few Lyman lines or even only Ly α , and often these lines are badly saturated so $N(\text{H I})$ is highly uncertain. Uncertain $N(\text{H I})$ measurements lead to uncertain metallicity measurements. With good constraints on metallicity and physical conditions, key properties such as mass and mass flow rates can be estimated.

2. Proof of Concept: First Results from *HST*

Galactic Winds Driven by Star Formation and AGN. The role of galactic outflows and “feedback” is one of the most pressing issues of current galaxy evolution studies. Some observations of objects such as Lyman-break galaxies, ULIRGs, and post-starburst galaxies have revealed dramatic outflows (e.g., Rupke et al. 2005, ApJS, 160, 87; Tremonti et al. 2007, ApJ, 663, L77; Steidel et al. 2010, ApJ, 717, 289). However, since these studies usually use the ULIRG or the post-starburst galaxy itself as the continuum source, they suffer from an ambiguity regarding the spatial extent, and hence the mass, of the outflow. These investigations also have a limited suite of diagnostics, e.g., Mg II or Na I and nothing else. By using absorption lines imprinted on background QSOs, these limitations can be overcome, and the EUV lines turn out to be particularly interesting. Multiple examples of different types of outflows are present in the sample COS data shown in Figure 1. For example, toward PG1206+459 we have clearly detected, at high significance, a doublet of Na IX at $z_{\text{abs}} = 1.0281$ (see the lowest panel in Fig. 1). Na IX has never been detected before, but this absorber is also detected in Ne VIII, Mg X, Ar VII, Ar VIII, and O V.

A possibly even more interesting outflow is detected at $z_{\text{abs}} = 0.9276$ in the PG1206+459 spectrum (Tripp et al. 2011, Science, 334, 952). From Fig. 1 we see that there is a dramatic cluster of absorption lines at this redshift detected in species such as S III and O III (middle and lower panels). This system is notable for the following reasons (see Tripp et al. for full details): First, we detect the adjacent suites of ions, including O III, O IV, O V, and O VI; N III, N IV, and N V; and S III, S IV, and S V. Second, we detect Ne VIII at very high significance. Third, the Ne VIII and N V velocity centroids are strongly correlated with the centroids of low ions such as Mg II, Si II, and C II (see Fig.3 in Tripp et al.). Fourth, while this absorption cluster is clearly a Lyman-limit absorber with many higher Lyman-series lines, the Lyman limit (LL) is not black and excellent $N(\text{H I})$ measurements can be obtained.

Finally, there is a post-starburst galaxy with an AGN at an impact parameter of 68 kpc from the sight line. These results have interesting implications: (1) The components in the cluster extend from -400 to $+1100$ km s $^{-1}$; with these velocities, some components must be exceeding the escape velocity of the galaxy. (2) Using the adjacent ions (e.g., SIII/SIV/SV) we can pin down the ionization state of each component and estimate their total column densities. Combined with the large impact parameter (70 kpc) to the galaxy, this implies that each component carries $\approx 10^8$ M $_{\odot}$ of mass in cool, photoionized gas, assuming a standard thin-shell model (e.g., Tremonti et al. 2007). Other geometries would give different masses, but an important mass component is implicated in any case. (3) However, the Ne VIII and N V must arise in hot gas that is correlated with the cool gas – Ne VIII/N V cannot originate in the cool photoionized gas. Moreover, this hot gas contains $10\times$ to $150\times$ more mass than the cool phase. In addition, the remarkable correspondence of the Ne VIII with lower ions suggests that the outflowing material is also interacting with a hotter (unseen) phase. How do species like Mg II and Si II survive at these outflow velocities embedded in such hot gas?

Cold Accretion of Pristine (Low-Metallicity) Gas. These spectra also reveal the opposite process: absorbers that are most naturally explained as cold, *inflowing* material, an equally important topic that is even more poorly constrained by observations. The partial Lyman limit absorber that produces the Lyman series lines shown in the top panel of Figure 1 is an example of apparently infalling, very metal poor gas. We have analyzed the metals affiliated with this partial Lyman limit system (Ribaudo et al. 2011, ApJ, 743, 207), and we find that the logarithmic metallicity is only $[\text{Mg}/\text{H}] = -1.71 \pm 0.06$. Moreover, we have spectroscopically identified and studied a nearby galaxy at the redshift of the Lyman limit absorber at an impact parameter of 37 kpc. Interestingly, that galaxy has a metallicity that is almost two orders of magnitude higher, $[\text{O}/\text{H}]_{\text{galaxy}} = 0.20 \pm 0.15$. This absorber may represent nearly primordial material that is accreting onto the galaxy via cold-mode accretion (Kereš et al. 2005), but other explanations remain viable. Subsequently, we studied all LL absorbers ($16.0 < \log N(\text{H I}) < 19.$) in our data combined with measurements from the *HST* archive and literature (Lehner et al. 2012, in prep.), and we find that 50% of LL have very low-metallicity ($Z \leq 0.03Z_{\odot}$). Our survey has tripled the sample of LL absorbers with good metallicity measurements at $z < 1$, but the sample is still small (28 systems total).

Requirements for a Future UV Telescope. Technical concepts are deferred to the second RFI, but the key technical requirements for this science can be briefly summarized. While *HST* has begun to observe QSO absorption lines at $\lambda_{\text{rest}} < 912$ Å, the number of $z_{\text{QSO}} = 1 - 2$ QSOs bright enough for *HST* is extremely small. To exploit this discovery space, a future UV spectrograph must have substantially better sensitivity than *HST*+COS, good spectral resolution (comparable to STIS and COS), and wavelength coverage down to at least 1150 Å and preferably down to ≈ 1000 Å.